Hindawi Publishing Corporation
Journal of Spectroscopy
Volume 2016, Article ID 2626414, 13 pages
http://dx.doi.org/10.1155/2016/2626414

Research Article

Optical Estimation on Pollution Level of Respirable Dust Based on Infrared Transmitting Behavior in Coalmine Fully Mechanized Working Face

Wen-Zheng Wang,[1,2] Yan-Ming Wang,[1,2] and Guo-Qing Shi[1,2]

[1]*Key Laboratory of Coal Methane and Fire Control, Ministry of Education, China University of Mining and Technology, Xuzhou 221116, China*
[2]*School of Safety Engineering, China University of Mining and Technology, Xuzhou 221116, China*

Correspondence should be addressed to Yan-Ming Wang; cumtwangym@163.com

Received 22 January 2016; Revised 9 March 2016; Accepted 20 March 2016

Academic Editor: Arnaud Cuisset

Respirable coal particle generated during underground mining is the main cause for gas-dust explosions and coal workers' pneumoconiosis (CWP) which needs accurate monitoring especially on its concentration. Focusing on the coal dust pollution in the fully mechanized working face of Huangbaici coalmine, coal particle was sampled for further industrial analysis and FT-IR test to obtain its chemical composition and optical constant. Combined with the simulated spatial distribution of airborne dust, the spectral transmission characteristics of coal dust within wavelengths of 2.5 to 25 μm under different operating conditions were obtained. The simulation results show that the transmittance and aerosol optical depth (AOD) of coal dust are closely linked and obviously influenced by the variation of dust generation source (intensity of dust release, position of coal cutting, and the wetting of the coal seam) and airflow field (wind speed and direction of ventilation). Furthermore, an optical channel of 1260–1280 cm^{-1} (7.937–7.813 μm) which is almost only sensitive to the variation of dust concentration but dull to the diameter change of coal dust was selected to establish the correlation of dust concentration and infrared transmittance. The fitting curve was then applied to retrieve the equivalent dust concentration based on optical information, and the comparison results demonstrate that the estimated pollution level is consistent with field measurement data in engineering practice.

1. Introduction

With the development of coal cutting mechanisms and ventilation technology, an increasing amount of coal is extracted from underground mines. A significant amount of coal dust is generated and dispersed into the mine atmosphere during coal crushing, extracting, exploding, and conveying in mining operations with the flow of the mine ventilation system [1–3]. Epidemiological studies have shown that exposure to coal dust is the main reason of coal workers' pneumoconiosis (CWP) [4]. Meanwhile, the presence of coal dust can be a serious explosion threat to coal mines which can cause a gas-dust explosion or coal dust explosion under certain conditions of temperature, oxygen concentration, and physical and chemical properties with or without methane [5]. The threat of coal dust is closely linked to the coal dust concentration in the whole working face which needs to be monitored continuously. Thousands of lives are lost because of coal dust related accidents every year in underground mines in China [6, 7]. Hence, it is critical to strengthen the theoretical and experimental research on the monitoring of dust concentration in underground coal mines to evaluate coal dust pollution in fully mechanized working face of coal mine.

Numerous studies have been carried out on the behavior of dust in a mine atmosphere; two main approaches are generally adopted to investigate the dust distribution in an underground coal mine, namely, field measurement and computer numerical simulation. The method of field measurement mainly depends on sampling and sampling analysis, which is

widely used for dust evaluation in an underground coal mine [8, 9]. However, the method of field measurement cannot monitor dust particles in real time in an underground coal mine. Meanwhile, it is difficult and costly for the field measurement method to give the variation of dust distribution under different working conditions and influencing factors. With the development of computer technology, computer numerical simulation in particular, the computational fluid dynamics (CFD) method has been widely used to study the dispersion and spatial distribution of dust particles in recent years [10]. Extensive CFD modeling work on dust dispersion in various workplaces in underground mines has been carried out considering different airflows, particle sizes, dust sources, and mechanisms of dust transport [11–13]. The numerical simulation results agree well with the field data, which can serve as a basis for evaluating and monitoring dust pollution in underground coal mines.

In recent years, particulate matter (PM) pollution in the open atmosphere has become more and more serious [14]. A great amount of research has been carried out to achieve accurate monitoring of PM, among which the optical detection technology is the most effective and widely used method [15, 16]. The attenuation and radiative transfer properties of PM including transmittance or aerosol optical depth can be obtained by satellite and ground-based optical remote sensing detection technologies which can be used as the optical signal to evaluate PM pollution [17]. The fully mechanized working face of the coal mine is a relatively confined cubic space that has a length that ranges from one hundred meters to thousands of meters; the optical sensing method can be modified and then adopted to monitor coal dust pollution in fully mechanized working face.

Nowadays, some portable instantaneous monitoring equipment and methods were used to evaluate dust pollution mainly based on the absorption and scattering properties of dust particle system in underground mine [18]. These kinds of portable monitoring equipment and methods mainly consider the dust particle system to be homogeneous and uniform in its detection space [19, 20]; actually, the dust concentration and diameter distribution are nonuniform which varies obviously especially in the whole fully mechanized working face. Meanwhile, the monitoring of dust particles through portable monitoring equipment is discrete and discontinuous. It is necessary to strengthen the study on the radiation and transfer characteristics of dispersion coal dust to achieve the accurate and real-time optical monitoring in the whole fully mechanized working face.

In this study, aiming at the coal dust pollution in the fully mechanized working face of Huangbaici coal mine which is located in Wuda coalfield, northwest China, the CFD method was adopted to simulate the spatial distribution of coal dust under different dust sources and airflow fields. Combined with Mie scattering and heat flux method, the radiation properties and transmission characteristics of coal dust in the fully mechanized working face of a coal mine under different influence factors were obtained and analyzed. Further spectral analysis was conducted to select the optical channel for dust concentration evaluation and finally an evaluation method of dust concentration in the fully mechanized working face of Huangbaici coal mine was presented.

2. Spatial Distribution of Coal Dust Hazard

2.1. Field Condition and Model Configuration. The Huangbaici coal mine in our study is located in the Wuda Coal District of Inner Mongolia Autonomous Region, northwest China [21]. The Wuda District holds a large amount of coal reserve which consists of coal-bearing strata of Pennsylvanian and Permian ages. Approximately, 80% of the coal mined in China comes from Pennsylvanian coal seams including Pennsylvanian Benxi Formation, the Pennsylvanian Taiyuan Formation, the Early Permian Shanxi Formation, and Xiashihezi Formation and the Late Permian Shangshihezi Formation [22, 23]. The fully mechanized working face of Huangbaici in our study is located at the NO. 15 coal seam of Pennsylvanian Taiyuan Formation. The width and height of the fully mechanized working face are 4 and 3 m, respectively, while the length varies dynamically with the advance of coal mining activity. The coal cutting machine and numerous kinds of supporting equipment and cable trays operate at the same time to ensure the safety of coal mining activity.

Based on the field condition of the fully mechanized working face of Huangbaici coalmine, a geometric model was set up for CFD simulation. Because of the complex working equipment in fully mechanized working face, it is impossible to establish an exact geometric model. Thus, the geometric model was simplified to be a cuboid calculation area of 100 m $*$ 4 m $*$ 3 m, a coal cutting machine of 5 m $*$ 2 m $*$ 1.2 m, with the supporting equipment represented by four cylinders with heights of 4 m and diameters of 0.15 m.

The air-dust coupled flow mathematical description was established to study the dispersion and distribution of coal dust particles in a fully mechanized working face. Three-dimensional steady incompressible Navier-Stokes equations were adopted to describe the airflow in a mine atmosphere. The k-ε model of Reynolds was applied to describe the turbulence effect, ignoring heat transfer. Given that the airflow model was established, a discrete phase model (DPM) was adopted to take dust movement into account, tracking dust movement by solving a differential equation for a discrete second phase in Lagrangian time. The second phases are spherical particles that are dispersed in a continuous phase. This model considers the coupling effect between the phases and its impact on both the discrete phase trajectories and the continuous phase flow. Such mathematical model and equations have been established in our previous study [24].

2.2. Simulation Performance and Result. In order to determine the simulation parameter and validate our CFD simulation results, coal dust distribution in the fully mechanized working face of Huangbaici coal mine was measured and obtained by field measurement method. According to the GB5748-85 (determination method of dust in the air of workplace) jointly issued by the Ministry of Health and Ministry of

Labor and Personnel of China [25], the concentration of rock dust can be determined when rock dust was sampled based on the weight gain of membrane and the intake air volume into Filter Dust Analyzer as follows $S = (W_2 - W_1)/Q_N$, where S is the concentration of rock dust, W_1 and W_2 are the weight of membrane before and after sampling, and Q_N is the intake air volume into Filter Dust Analyzer. The dust concentration distribution along the fully mechanized working face at three heights (0.5 m, 1.5 m, and 2.5 m) was obtained. Meanwhile, the coal dust particle generated in coal cutting area was sampled to obtain its diameter distribution by further analysis in laboratory. The dust diameter distribution test was carried out by graded sieves with different mesh. The test results of dust diameter distribution by quality at the generation source in fully mechanized working face are as follows: 0–5 μm (11.94%), 5–10 μm (14.69%), 10–20 μm (24.84%), and >20 μm (48.53%).

Thus, a typical simulation based on the normal condition in underground working face was conducted whose main parameters and boundary conditions were determined as follows. The coal dust in the simulation was bituminous coal particles, whose diameter distribution by quality is 0–5 μm (10%), 5–10 μm (15%), 10–20 μm (25%), 20–50 μm (30%), and >50 μm (20%) as tested in our experiment with a flow rate of 0.01 kg/s. The inlet boundary type was set to be a velocity inlet with a magnitude of 2.5 m/s. The direction of ventilation is positive. The coal cutting machine is 5 m away from the intake of working face. The outlet boundary type was set to be outflow. The DPM condition and shear condition of the walls were set to be rebound with a recovery coefficient of 0.25 and no slip, respectively.

By conducting the CFD simulation, the distribution of the coal dust concentration and diameter in the central axis (1.5 m high) along the fully mechanized working face was obtained. Since the dust diameter distribution is an important input in Mie scattering model, which needs integral processing for number density function as nonuniform particles as shown in (3) and (4), then, the Rosin-Rammler function which is widely used in the statistics of coalmine dust particles [26, 27] was adopted in our study. The diameter distribution of coal dust was represented by the Rosin-Rammler function $W(D)$ [28]; R^2 is the correlation coefficient of the Rosin-Rammler function:

$$W(D) = 100 \exp\left(-\beta * D^n\right), \quad (1)$$

where $W(D)$ is the Rosin-Rammler function representing the cumulative distribution of the quality of coal particles greater than a certain diameter D and β and n are the coefficients related to the diameter distribution of coal particles. The numerical results of coal dust dispersion were shown in Table 1.

The dust diameter distribution at every sampling point was fitted to Rosin-Rammler function which can be further used in Mie scattering model as handled in (6). Meanwhile, the correlation coefficient of the fitting at every sampling point was also given.

Then, the simulation results of dust concentration distribution were validated by our field measurement result as described above. Adopt the dust concentration distribution at 1.5 m height along the working face to analyze the difference, as presented in Figure 1.

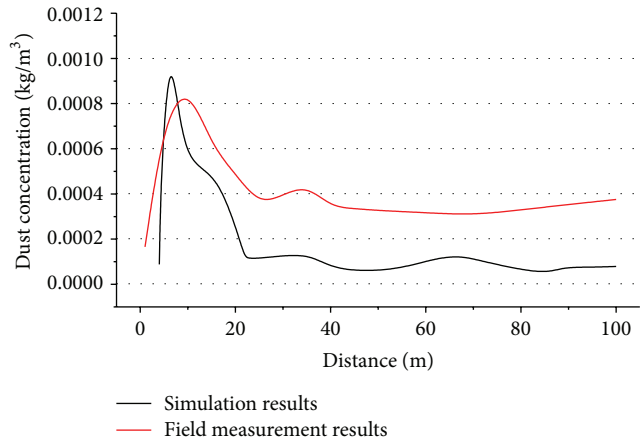

Figure 1: Validation of CFD simulation results by field measurement.

Figure 1 presents that both the simulation results and field measurement results are firstly increased sharply with the increase of distance and then drop dramatically until 25 m; eventually, the dust concentration gradually keeps stable. This illustrates that the CFD simulation results and field measurement results agree well to a certain extent. However, the peak point of simulation result and field measurement result are a bit deviating, and an obvious difference on dust concentration can be observed when the dust concentration keeps stable especially when the distance comes to 25 m. This is mainly due to the fact that (a) the parameters in CFD simulation are controllable and constant, while, during field measurement, the wind speed may vary a little considering the working condition of fan and the dust release intensity may change a bit with the advance of coal cutting. The uncontrollable factor in field measurement is one of the reasons for such difference. (b) The CFD method just considers the main force between airflow and particles including drag force, gravity, Saffman lift force, thermophoresis force, and brown force. But the interaction of airflow and particles, the rebound of dust particles on ground and wall, the influence of water on dust particles sedimentation (the humidity is quite high in underground coalmine), and the influence of dust particles on airflow are hard to consider but important. The combined effect of these factors results in the difference of dust concentration when distance comes to 25 m. As a whole, the CFD simulation gives an acceptable result especially when considering that it is hard and costly to conduct field measurement under different working conditions (different wind speed, dust release intensity, direction ventilation, etc.).

Apart from the calculation above, the distribution of coal particles under different intensities of dust release (0.002, 0.005, and 0.01 kg/s), different positions of coal cutting (coal cutting machine 5, 30, and 60 m from intake), different wettings of coal seams (original coal seam and coal seam of water injection), different wind speeds (1, 2.5, and 4 m/s), and different directions of ventilation (positive and negative

Table 1: Distribution of the coal particle concentration and diameter.

Distance/m	Dust concentration/(kg/m^3)	Diameter distribution by Rosin-Rammler $W(D) = 100\exp(-\beta * D^n)$		
		β	n	R^2
4.0	$8.83E-05$	0.0125	1.0103	0.9718
4.4	$5.31E-04$	0.0261	0.8960	0.9733
6.2	$1.04E-03$	0.0294	0.8173	0.9744
8.0	$7.68E-04$	0.0101	1.0873	0.9871
10.2	$5.24E-04$	0.0201	0.9932	0.9905
16.4	$4.92E-04$	0.0230	0.9565	0.9876
21.8	$1.35E-04$	0.0198	1.0012	0.9877
22.2	$1.10E-04$	0.0156	1.1846	0.9838
27.6	$1.21E-04$	0.0146	1.4109	0.9753
35.8	$1.37E-04$	0.0185	1.2583	0.9764
40.6	$5.96E-05$	0.0322	1.0115	0.9730
53.2	$5.83E-05$	0.0217	1.1752	0.9878
62.0	$1.17E-04$	0.0246	1.1307	0.9865
67.6	$1.26E-04$	0.0480	0.9245	0.9490
71.6	$1.03E-04$	0.0506	0.9608	0.9509
84.8	$4.22E-05$	0.0434	1.0070	0.9632
88.6	$7.58E-05$	0.0212	1.4730	0.9781
94.6	$7.56E-05$	0.0259	1.3287	0.9794
100.0	$7.95E-05$	0.0095	1.6982	0.9865

ventilation) were also simulated; the calculation results of dust distribution were further used in the simulation of transmission properties under different influencing factors in Section 4.

3. Complex Refractive and Transmission Properties of Coal Dust

3.1. Scattering and Optical Constants of Coal Dust Particles. The dispersion and distribution of coal dust particles in the fully mechanized working face of a coal mine can be obtained according to the simulation of the air-dust coupled flow mathematical model. Based on the simulation results of the coal dust distribution, a Mie scattering model was adopted to obtain the spectral radiation characteristics at wavelength λ of coal dust particles [29]:

$$Q_e(m,\chi) = \frac{C_e}{G} = \frac{2}{\chi^2}\sum_{n=1}^{\infty}(2n+1)\,\mathrm{Re}\left(a_n + b_n\right) = \frac{4}{\chi^2}\,\mathrm{Re}\left\{S_0\right\} \quad (2)$$

$$Q_s(m,\chi) = \frac{C_s}{G} = \frac{2}{\chi^2}\sum_{n=1}^{\infty}(2n+1)\left[\left|a_n\right|^2 + \left|b_n\right|^2\right],$$

where m is the optical constant of particle $m = n - ik$, n and k are the refractive index (single refractive index) and absorption index, respectively, χ is the size parameter $\chi = \pi D/\lambda$, G is the geometric projection area of the spherical particle $G = \pi D^2/4$ (μm^2), Re is the real component of complex number, a_n and b_n are the Mie scattering coefficients, and S_0 is the prior amplitude functions.

Table 2: Industrial and elemental analysis of coal particles.

Industrial analysis (%)				Elemental analysis (%)					
M	A	V	Fc	C	H	O	N	S	Others
2.67	24.96	29.63	42.74	58.53	3.60	9.09	0.84	0.31	27.63

The scattering calculation of coal dust requires both the spatial distribution and the optical constants of coal particles. Thus, the coal dust particles were sampled from the fully mechanized working face of Huangbaici coal mine which is located in Wuda coalfield, northwest China. Then, the industrial and elemental analysis and FT-IR experiment were conducted on the coal particles sampled in underground coal mine to obtain the chemical composition and spectral transmittance of coal dust, as shown in Table 2 and Figure 2. The experimental method and equipment of the industrial analysis and FT-IR test for rock dust have been given in our previous study [30].

Thus, the coal dust particles in the fully mechanized working face can be determined to be bituminous coal particles according to the degree of coal metamorphism based on the industrial and elemental analysis of the coal sample.

In order to conduct FT-IR test, the sampled coal dust particles were firstly pulverized to less than 200 mesh (74 μm) and dried at 105°C for 4 h according to the requirement of

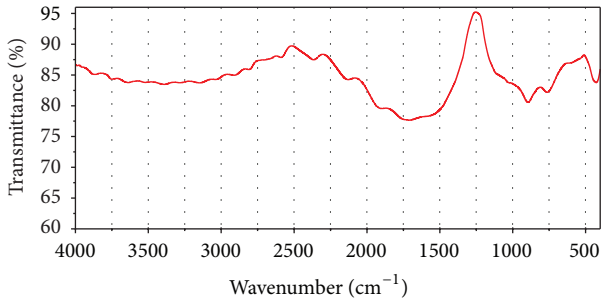

Figure 2: Spectral transmittance of coal dust from FT-IR test.

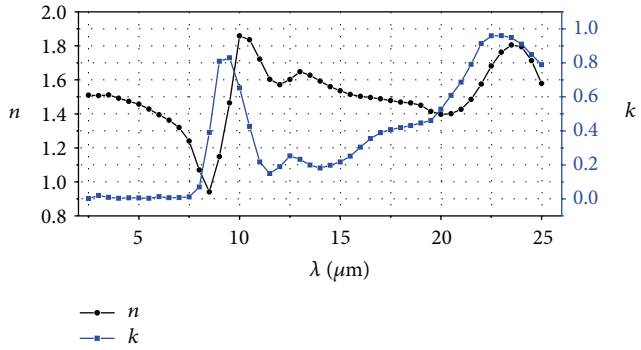

Figure 3: The optical constant of coal particles.

FT-IR test. Then, coal dust particles were suspended and pressed in a KBr matrix with the thickness of 1 mm and the proportion of 1 : 100 under the pressure of 10 t/cm^2 for 3 min. The well prepared KBr matrix was subsequently measured on its spectral transmittance within the spectral region 400–4000 cm^{-1}, as shown in Figure 2. The FT-IR equipment used in this test is Bruker Vertex 80v which is manufactured in Germany. The main performance indexes of Bruker Vertex 80v are as follows: spectral range, 8000–350 cm^{-1}; spectral resolution, 0.06 cm^{-1}; sensitivity, under the condition of full spectrum of linear accuracy better than 0.7%, peak-peak noise value < 8.6×10^{-6} Abs, signal-to-noise ratio better than 55000 : 1 (peak to peak); linearity, 0.07%; interferometer, high precision dynamic calibration Mayer interferometer.

Based on the spectral transmittance of coal dust particles, combined with the properties of KBr matrix preparation, Kramers-Kronig (K-K) relation was adopted to retrieve the optical constant of rock index [31, 32]. Through the simulation, the optical constant of bituminous coal dust was obtained as shown in Figure 3.

3.2. Transmitting Behavior of Coal Dust. The particle swarms of coal dust in any location along the fully mechanized working faces are composed of a series of different scale particles. The optical radiation parameters of a nonuniform particle swarm can be given by the following formula:

$$\beta = \int_0^\infty C_e(D)\, N(D)\, dD \tag{3}$$

$$\sigma_s = \int_0^\infty C_s(D)\, N(D)\, dD \tag{4}$$

$$\omega = \frac{\sigma_s}{\beta}, \tag{5}$$

where D is the diameter of particle, μm; $C_e(D)$ and $C_s(D)$ are the attenuation and scattering cross section of a particle with a diameter of D; $N(D)$ is the particle number density distribution, in m$^{-3} \cdot \mu$m^{-1}; and ω is the scattering albedo:

$$N(D) = -\frac{dW(D)}{dD} \cdot \frac{\rho_a}{\rho_b (4/3)\pi D^3}, \tag{6}$$

where ρ_a and ρ_b are the quantity concentration of the total dust and actual density of coal, respectively. Because of the common industrial analysis of coal dust, nonuniform particles are generally divided into several size ranges for statistics. Then, discrete integration was employed to approximate the Rosin-Rammler function in this paper, and the middle diameters of each particle group were selected as equivalent diameters for calculation to approximate the above equations.

Based on the optical scattering and extinction properties of coal dust obtained from Mie scattering calculation, aimed at the transmission characteristics and aerosol optical depth (AOD) of dust particles, the numerical method of radiative transfer was applied [33–38]. Here, considering a gray medium condition, the one-dimensional radiative transfer equation (RTE) at the wavelength λ on the direction θ can be written as follows:

$$\cos\theta \frac{dI(\tau)}{d\tau} = (1-\omega) I_b(\tau) - I(\tau) + \frac{\omega}{2} \int_0^\pi I(\tau, \theta_i)\, \Phi(\theta, \theta_i) \sin\theta_i\, d\theta_i, \tag{7}$$

where τ is the spectral optical thickness; I is the intensity of the radiation, in W/(m^2·sr); and I_b is the radiation intensity of blackbody. Considering isotropic scattering ($\Phi \equiv 1$), the two-flux method was applied to calculate and analyze the spectral radiation intensity and spectral transmission characteristics of the dust particle system in a one-dimensional direction [39]. Assume the radiation intensity in positive and negative directions to be a constant value and assume it has nothing to do with the angle. Thus,

$$\begin{aligned} \frac{1}{2}\frac{dI^+}{d\tau} &= (1-\omega) I_b - I^+ + \frac{\omega}{2}(I^- + I^+) \\ -\frac{1}{2}\frac{dI^-}{d\tau} &= (1-\omega) I_b - I^- + \frac{\omega}{2}(I^- + I^+). \end{aligned} \tag{8}$$

The corresponding boundary conditions are $I^+ = 0$ for $\tau = 0$ and $I^- = 0$ for $\tau = \tau_L$; I^- and I^+ are the radiation intensities in positive and negative direction, respectively, in W/(m^2·sr). Then, the average apparent transmittance of coal dust at the wavelength λ can be given as

$$\gamma = \frac{2\pi I^+}{E_b}, \tag{9}$$

where E_b is the radiation of blackbody.

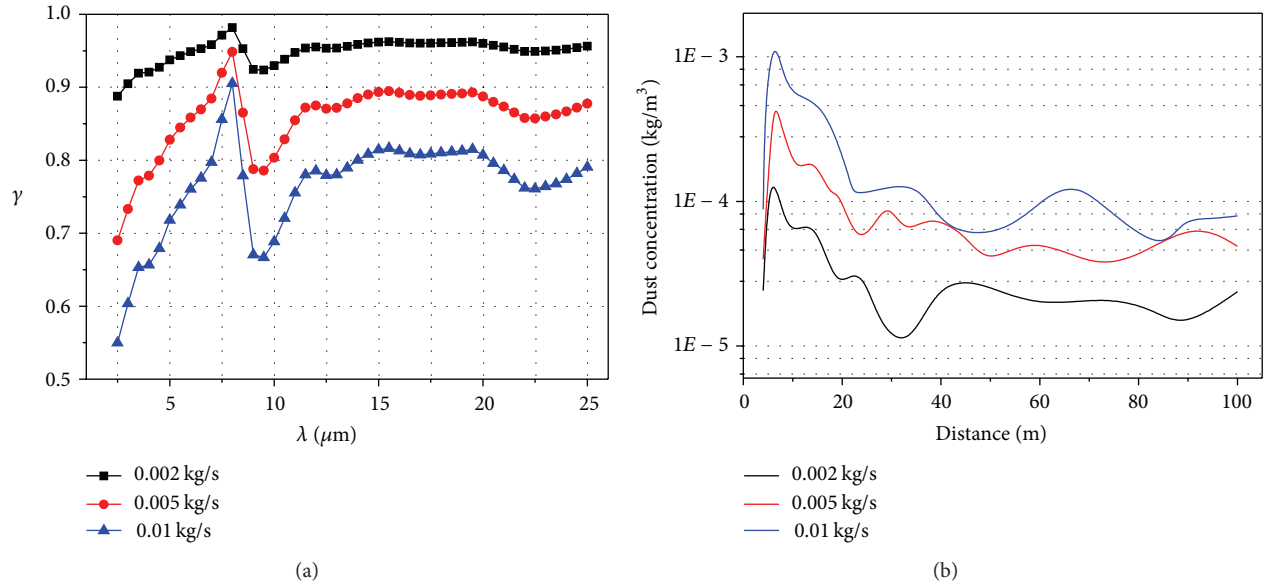

Figure 4: Influence of the dust release intensity on (a) spectral transmittance and (b) dust concentration.

4. Results of Dust Optical Characteristics under Different Operating Conditions

The distribution of coal particles in a fully mechanized working face is mainly affected by the dust source and airflow field. Aimed at different influencing factors of the dust source (intensity of dust release, position of coal cutting, and the wetting of the coal seam) and airflow field (wind speed and direction of ventilation), combined with the optical constant of coal dust in Figure 2, the transmission characteristics and AOD of the coal particles were simulated and analyzed by solving Mie scattering model and heat flux method. The optical constant of coal dust obtained and the radiative transfer equation solved are all at the ambient temperature (300 K) of underground coal mine.

4.1. Influence of the Intensity of Dust Release. The intensity of coal dust release is closely linked to the cutting speed, cutting depth, and lead angle of the coal cutting machine, which further affects the distribution of the coal particles in fully mechanized working face. Based on the CFD simulation results of dust distribution under different dust release intensities (0.002, 0.005, and 0.01 kg/s) in combination with the heat flux method, the transmission characteristics of coal particles were calculated and analyzed.

As can be seen from Figure 4(a), the transmittance of coal dust increases sharply with the increasing wavelength, reaching a maximum at 8 μm and then decreasing rapidly, reaching a minimum at 9.5 μm. Eventually, the transmittance rises gently and remains stable when the wavelength is 12 μm. The transmittance is obviously decreased with increasing dust release intensity; the degree of decrease is relatively much smaller for 8 μm. This is because the concentration of coal dust is greatly increased with increasing dust release intensities, as seen from Figure 4(b), resulting in the weakened transmission characteristics of coal particles in Figure 4(a). The spectral transmittance is the strongest for 8 μm, which weakens the influence of dust concentration, thus causing the degree of transmittance decrease that is relatively much smaller for 8 μm.

4.2. Effect of the Position of Coal Cutting. With advances in coal mining activities in a fully mechanized working face, a coal cutting machine would move from one side of the coal seam to another side. Coal particles generated during the process of coal cutting mainly disperse in the downward airflow of the coal cutting machine; the atmosphere in the upward airflow of the coal cutting machine is mainly fresh air with few contaminants (the dust concentration was set to be 1×10^{-5} kg/m^3 according to Wang and Ren [1]). Thus, three positions of coal cutting (coal cutting machine is 5, 30, and 60 m from the intake of the working face) were adopted in this section to simulate the transmission characteristics of the coal particles. The transmittance of coal dust under the position of coal cutting that is 30 m from the intake is divided by that of 5 m and 60 m to obtain the dimensionless ratio ($\gamma_{5\,\mathrm{m}}/\gamma_{30\,\mathrm{m}}$ and $\gamma_{60\,\mathrm{m}}/\gamma_{30\,\mathrm{m}}$) for further analysis, as shown in Figure 5.

Figure 5(a) shows that the dimensionless ratio $\gamma_{5\,\mathrm{m}}/\gamma_{30\,\mathrm{m}}$ is less than 1, while the ratio $\gamma_{60\,\mathrm{m}}/\gamma_{30\,\mathrm{m}}$ is greater than 1 under the waveband of 2.5 to 25 μm, which indicates that the transmittance characteristics are increased with the advance of coal mining activity. This is because, with the advance of coal mining activity, the coal cutting machine gradually moves from the intake to the outtake of the working face; the downwind region is heavily polluted by coal dust and is gradually diminished but the upwind region, which is relatively fresher, is enlarged, causing the decrease of coal dust pollution as a whole in a fully mechanized working face.

An obvious trend that approximates a constant value of 1 is observed at the waveband from 7 to 9 μm for $\gamma_{5\,\mathrm{m}}/\gamma_{30\,\mathrm{m}}$

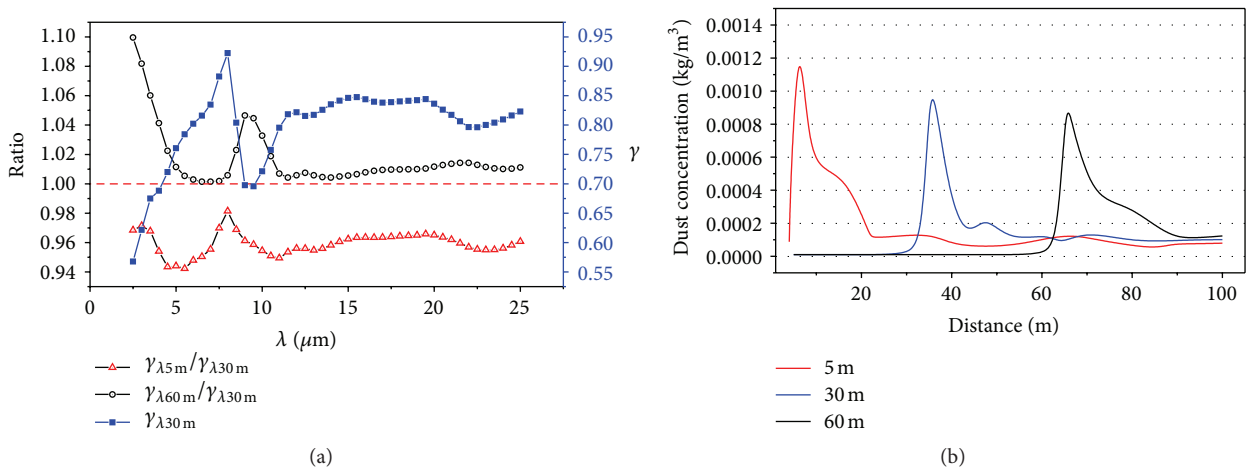

Figure 5: Effect of the position of coal cutting on (a) spectral transmittance and (b) dust concentration.

and from 6 to 8 μm for $\gamma_{60\,m}/\gamma_{30\,m}$, indicating that variations of transmittance with different coal cutting positions are weakened. This is because the spectral transmittance of coal dust is the strongest at the wavelength of approximately 8 μm; the influence of dust distribution on transmission characteristics is obviously reduced at 8 μm compared to other wavebands.

4.3. Impact of Wind Speed and the Wetting of the Coal Seam on AOD. The ventilation system of a coal mine mainly aims to provide fresh air for the underground workers by carrying contaminants (e.g., methane, carbon monoxide, and dust) away from the coal mine. Coal particles spread outwards in a fully mechanized working face, mainly relying on the effect of airflow. Meanwhile, wetting technology has been widely used in most coal mines by water injection before the extraction of the coal seam. Relevant studies have shown that the distributions of coal particles' concentration and diameter are directly affected by wind speed and the use of water injection technologies, further affecting the transmission characteristics of coal particles. The speed of airflow in a fully mechanized working face is confined within 0.25 to 4 m/s according to the safety regulations in coal mines in China. Thus, with the original coal seam under different wind speeds (1, 2.5, and 4 m/s) and the wetting coal seam under wind speed of 2.5 m/s, the AOD of coal particles was simulated and analyzed, as shown in Figure 6.

Figure 6 indicates that the AOD of coal dust is obviously decreased with the increasing wind speed in a fully mechanized working face. This is because airflow is the main cause for the outward spread of coal particles; the settlement of coal particles under different wind speeds varies greatly when there is an optimal speed for dust settlement. Before the optimal speed, coal particles are more prone to settle with increasing wind speed. All of the wind speeds (1, 2.5, and 4 m/s) that were set up in our study are under the optimal speed presented in Figure 7(a), causing a decreased distribution of coal dust as well as a decreased AOD of coal particles.

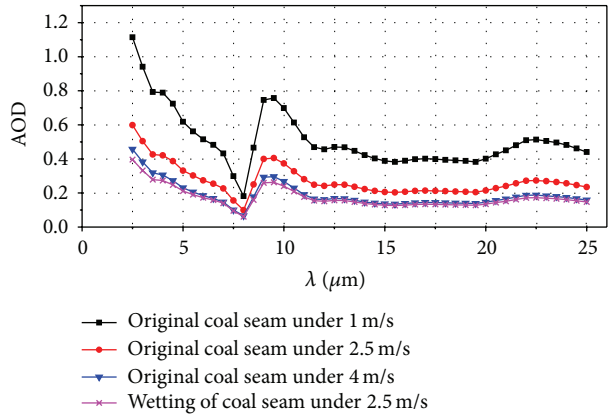

Figure 6: Spectral AOD of coal dust under different wind speeds and wettings of the coal seam.

The AOD of coal particles is obviously decreased by adopting the water injection technology of the coal seam. The moisture of the coal seam can be increased with the use of water injection technology, which is against the generation of coal particles during the process of coal cutting. Small particles can form larger particles under the effect of increased moisture causing much easier settlement. Thus, the concentration of coal particles in Figure 7(b) is decreased with the use of water injection technology, resulting in the decreased AOD of coal particles in the fully mechanized working face.

4.4. Effect of the Direction of Ventilation on AOD. The ventilation in the fully mechanized working face can be divided into positive ventilation and negative ventilation considering the direction of coal cutting and airflow. The coal cutting and airflow have the same direction for positive ventilation and the opposite direction for negative ventilation. Based on the CFD simulation results under positive and negative ventilation, the AOD of coal particles in the fully mechanized

Table 3: Spectral AOD versus direction of ventilation.

λ/μm	AOD Positive direction	AOD Negative direction	λ/μm	AOD Positive direction	AOD Negative direction	λ/μm	AOD Positive direction	AOD Negative direction
3	0.52062	0.60375	11	0.28086	0.31968	19	0.20359	0.23151
4	0.43089	0.49614	12	0.23811	0.27075	20	0.21137	0.2406
5	0.33751	0.38509	13	0.24519	0.2788	21	0.23871	0.27215
6	0.27493	0.31253	14	0.21768	0.2472	22	0.27067	0.30879
7	0.21937	0.24891	15	0.2002	0.22729	23	0.26736	0.30463
8	0.09544	0.10727	16	0.20257	0.23017	24	0.25376	0.28889
9	0.40835	0.47070	17	0.21023	0.23911	25	0.23153	0.26354
10	0.37973	0.43616	18	0.20673	0.23511			

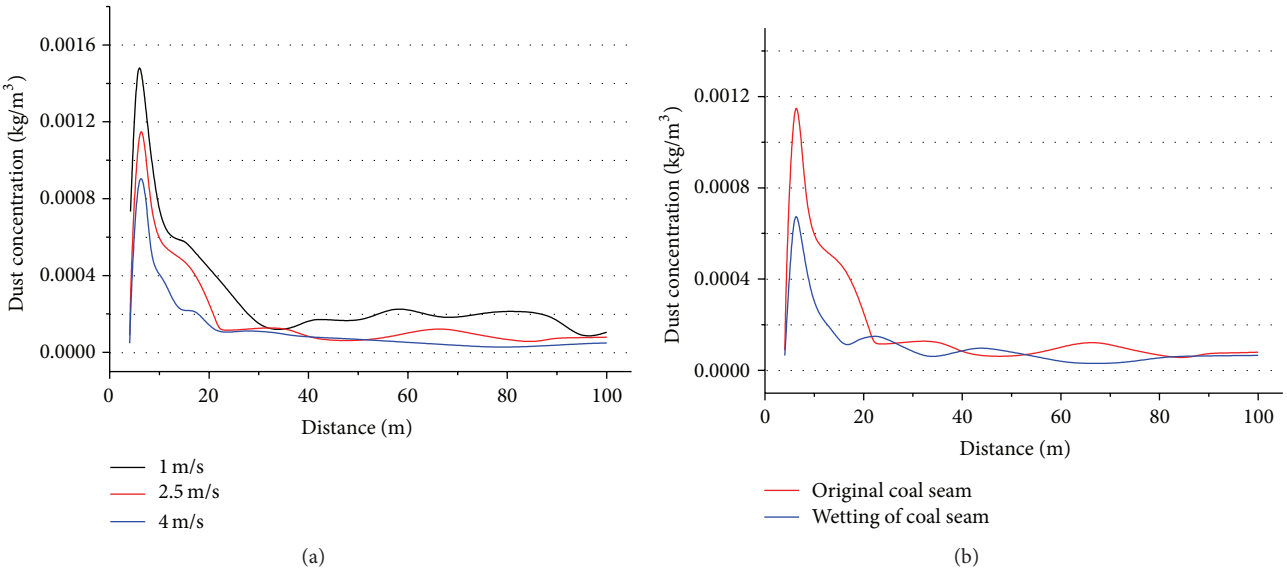

Figure 7: Dust concentration under different (a) wind speeds and (b) wettings of the coal seam.

working face was simulated and analyzed, as presented in Table 3.

Table 3 shows that the AOD of coal particles under positive and negative directions has a similar variation law versus wavelength. However, the AOD under positive ventilation is slightly weaker than that under negative ventilation. This is because the turbulence effect of airflow would be slightly enhanced under negative ventilation as a whole, which is against the settlement of coal dust; the average concentration of coal dust is $1.90E-4\,\text{kg/m}^3$ for negative ventilation and is $1.307E-4\,\text{kg/m}^3$ for positive ventilation, as seen from Figure 8.

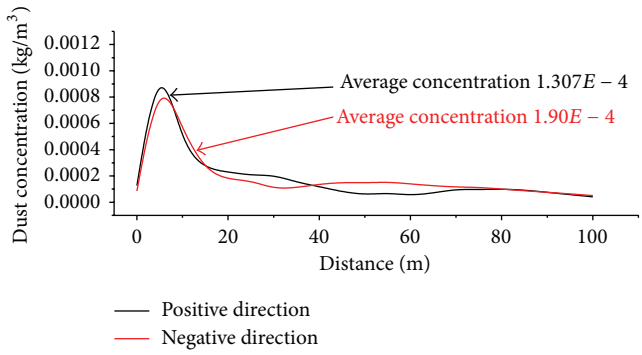

Figure 8: Dust concentrations under different directions of ventilation.

5. Waveband Selection and Field Application

As can be concluded from the simulation and analysis above, the transmission properties of coal dust in fully mechanized working face vary obviously under different working conditions and influencing factors which reflect the variation of the dust concentration and dust diameter distribution in essence. An anomalous point of transmittance around 8 μm was observed in Section 4 which varies minimally under different influencing factors. Aiming at the evaluation of dust concentration level in the whole working face, the influencing effect of dust diameter on the transmittance signal should be determined first.

5.1. Influence of Dust Diameter on Transmittance. To study the influence of diameter, a formula, $\gamma_{\text{ratio}\cdot s} = (\gamma_m - \gamma_s)/\gamma_m$,

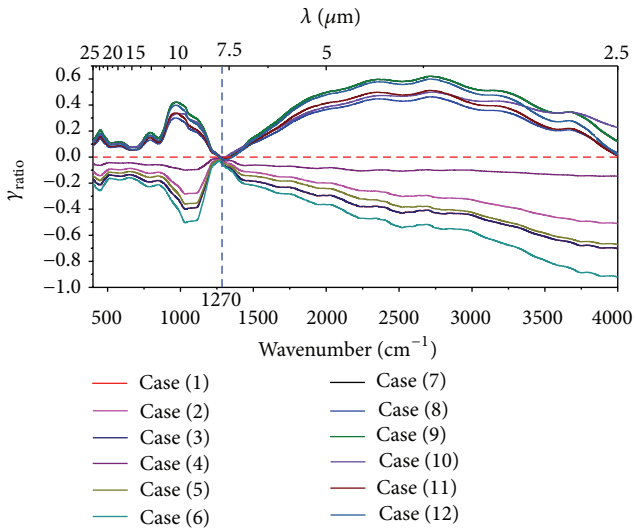

Figure 9: Influence of diameter on transmittance under different cases (uniform dust diameter, dust release intensity, position of coal cutting, wind speed, whether there is wetting of coal seam or not, and direction of ventilation): (1) 5 μm, 0.005 kg/s, 5 m, 2.5 m/s, no, positive; (2) 5 μm, 0.005 kg/s, 5 m, 4 m/s, no, positive; (3) 5 μm, 0.01 kg/s, 5 m, 2.5 m/s, no, positive; (4) 5 μm, 0.005 kg/s, 5 m, 2.5 m/s, yes, positive; (5) 5 μm, 0.005 kg/s, 30 m, 2.5 m/s, no, positive; (6) 5 μm, 0.005 kg/s, 5 m, 2.5 m/s, no, negative; (7) 50 μm, 0.005 kg/s, 5 m, 2.5 m/s, no, positive; (8) 50 μm, 0.005 kg/s, 5 m, 4 m/s, no, positive; (9) 50 μm, 0.01 kg/s, 5 m, 2.5 m/s, no, positive; (10) 50 μm, 0.005 kg/s, 5 m, 2.5 m/s, yes, positive; (11) 50 μm, 0.005 kg/s, 30 m, 2.5 m/s, no, positive; (12) 50 μm, 0.005 kg/s, 5 m, 2.5 m/s, no, negative.

was put forward, where $\gamma_{\text{ratio}\cdot s}$ represents the influence of the transmittance of coal dust with uniform diameter (γ_s) on that of a mixture of dust (γ_m), γ_m is the transmittance of mixture dust, and γ_s is the transmittance of coal dust with uniform diameter (5 μm (representing small particle) and 50 μm (representing large particle)) based on the same concentration of the CFD simulation. The influence of dust diameter on transmittance under different working conditions and influencing factors was calculated and summarized, as shown in Figure 9.

Figure 9 indicates that the spectral variations of $\gamma_{\text{ratio}\cdot s}$ under different intensities of dust release and wind speed are similar, except for the difference in concrete magnitude. $\gamma_{\text{ratio}\cdot 5\,\mu\text{m}}$ under different intensities of dust release and wind speed are all positive, while $\gamma_{\text{ratio}\cdot 50\,\mu\text{m}}$ are all negative, which indicates that the transmittance of coal dust is obviously enhanced with increasing diameter under the same distribution of dust concentration. With the decrease of the dust release intensity and the increase of wind speed, the spectral variations of $\gamma_{\text{ratio}\cdot s}$ gradually become relatively stable.

The spectral variations of $\gamma_{\text{ratio}\cdot s}$ fluctuate greatly under wavebands of 400–4000 cm^{-1} (25–2.5 μm) among which an anomalous waveband around 1270 cm^{-1} whose absolute value reaches the minimum point of zero (all within 0.05) can be obviously observed. Such waveband indicates that the transmittance of coal dust is almost not sensitive to the variation of dust diameter under around 1270 cm^{-1}; considering the variation of transmittance under different influencing factors listed in Section 4 under around 1270 cm^{-1}, it can be deduced that the transmittance is the only function of dust concentration under the permissible error for engineering application.

5.2. Correlation of Dust Concentration and Infrared Transmittance. According to the above discussions, the optical channel of 1260–1280 cm^{-1} (7.937–7.813 μm) is selected in this case study to evaluate the dust concentration level in fully mechanized working face; for that, the transmission signal is almost only sensitive to the variation of dust concentration. By adopting the equivalent transmittance within the optical channel of 1260–1280 cm^{-1} (7.937–7.813 μm) and equivalent dust concentration of the whole working face, the variation law of dust concentration and the optical transmittance in whole working face was further calculated and analyzed. Here, considering the irrelevance between the transmittance within 1260–1280 cm^{-1} and particle size as demonstrated in Figure 9, a mean diameter 20 μm representing the nonuniform particles was adopted in the Mie calculations according to the analysis in Section 2.2. The equivalent transmittance within 1260–1280 cm^{-1} (7.937–7.813 μm) can be calculated by

$$\overline{\gamma} = \frac{\int_{\lambda_1}^{\lambda_2} \gamma E_b d\lambda}{\int_{\lambda_1}^{\lambda_2} E_b d\lambda}. \tag{10}$$

The dust concentration can be obtained by the one-to-one relationship between dust concentration and optical transmittance presented in Figure 10(a) if the optical transmittance was determined. Meanwhile, considering dust suppression method and equipment, there is a maximum limit of dust concentration in the working face. Thus, only some points marked in Figure 10(a) are valid which can be used for the evaluation of dust concentration in underground working face. The invalid points exceed the dust concentration level in working face which is useless and meaningless in this study. Further analysis on the valid data was conducted by fitting the curve to obtain the corresponding function, as shown in Figure 10(b).

For the engineering application, the function and control variables should not be too complex; meanwhile, the function must agree well with the curve and points. Thus, a polynomial with two polynomial orders was used to fit the curve and points in Figure 10(b). The fitting results agree well with the original points whose correlation coefficient reaches 0.99995 and the residual sum of squares is $1.04373E-4$. Thus, an effective fitting function was put forward and given as follows:

$$C = 2.06214 * \overline{\gamma}^2 - 6.44759 * \overline{\gamma} + 4.39114. \tag{11}$$

5.3. Field Application in Huangbaici Coal Mine. Simulation study gives the function of dust concentration and optical transmittance under the optical channel of 1260–1280 cm^{-1} (7.937–7.813 μm) for its dullness of dust diameter variation.

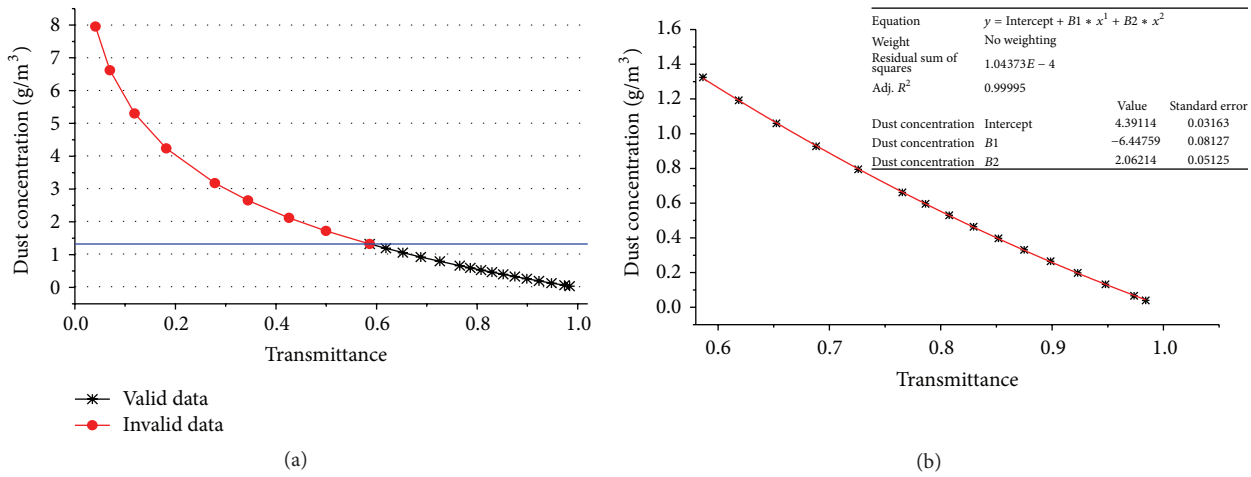

Figure 10: The correlation between dust concentration and transmittance.

Table 4: Dust concentration distribution along the working face.

Distance/m	Dust concentration/(g/m^3)		
	0.5 m	1.5 m	2.5 m
1	0.24021	0.16605	0.06150
5	0.74450	0.72991	0.12454
10	0.93809	0.88750	0.19890
15	0.51265	0.61281	0.24133
20	0.41177	0.48878	0.29447
25	0.32211	0.35261	0.32579
30	0.33073	0.39576	0.33696
35	0.33935	0.43890	0.34812
40	0.32293	0.34323	0.28529
45	0.31482	0.33517	0.28121
50	0.30671	0.32711	0.27713
60	0.29748	0.31686	0.27264
70	0.28825	0.30661	0.26816
80	0.30564	0.32971	0.26749
90	0.32303	0.35282	0.26683
100	0.34042	0.37592	0.26617

Then, the fitting function obtained was used in field underground working face of Huangbaici coal mine to evaluate the dust concentration level.

The field measurement experiments on coal dust distribution have been carried out and described in Section 2.2. Then, the coal dust distribution measured samples at three heights above the ground (0.5 m, 1.5 m, and 2.5 m) were shown in Table 4.

Based on the field data of dust distribution in three sampling lines (0.5 m, 1.5 m, and 2.5 m high along the working face), the optical transmittance of the three lines was calculated. The transmittance within the optical channel of 1260–1280 cm^{-1} (7.937–7.813 μm) was listed in Table 5.

Then, the equivalent transmittance of three lines was loaded into (11) to retrieve the equivalent dust concentration in the fully mechanized working face. Meanwhile, the equivalent dust concentration was also directly calculated from the field data. The directly calculated dust concentration and retrieved dust concentration were compared to get the relative error, as listed in Table 6.

The retrieved data is a little greater than field data but all within the relative error of 0.1. The error is mainly due to the fact that the transmittance within optical channel of 1260–1280 cm^{-1} (7.937–7.813 μm) is still slightly influenced by the diameter distribution which cannot be totally removed. Meanwhile, small error still exists in the fitting function which is hard to eliminate especially for engineering application. However, such results with all the relative errors within 0.1 can also be accepted for engineering application which can be used for dust concentration evaluation in the fully mechanized working face of Huangbaici coal mine.

5.4. Limitation of the Methodology for Retrieving Dust Concentration. The coal dust concentration in underground working face can be retrieved by the methodology presented in this paper. Meanwhile, obvious shortcomings and limitations still exist concerning this method mainly including the following: (a) the optical channel of 1260–1280 cm^{-1} (7.937–7.813 μm) was adopted in this study to correlate dust concentration and transmittance, when dust concentration is high to a certain extent which may cause the optical signal to be invalid. Such occasion does not exist because there is a maximum limit of dust concentration under normal mining conditions that cannot lead the optical signal to be invalid which have been discussed in Section 5.2. Meanwhile, when the dust concentration is low to a certain extent which leads to quite high transmittance, in this occasion, the transmittance is not sensitive to the variation of dust concentration. Take transmittance 0.995 as an example; according to our correlation, the equivalent dust concentration was obtained as low as 0.01735 g/m^3 (17.35 mg/m^3). When dust concentration is lower than 0.01735 g/m^3 which may be caused by lower dust release intensity, larger wind speed, or farther distance of coal cutting from the intake, it is hard to detect the variation of dust concentration from transmittance. (b) The

Table 5: The transmittance of coal dust under the optical channel of 1260–1280 cm^{-1}.

Height/m	Transmittance			
	1260 cm^{-1}	1270 cm^{-1}	1280 cm^{-1}	Equivalent
0.5	0.79357634	0.78322529	0.76093461	0.779245413
1.5	0.77153042	0.76953047	0.74345684	0.761505907
2.5	0.83354416	0.84187375	0.83086851	0.835428809

Table 6: The comparison of field data and retrieved data.

Height/m	Equivalent dust concentration/(g/m^3)		
	Field data	Retrieved data	Relative error
0.5	0.583638	0.619065	0.060700756
1.5	0.626850	0.677079	0.080129348
2.5	0.410757	0.443890	0.080663723

transmittance under 1260–1280 cm^{-1} (7.937–7.813 μm) was considered as the only function of dust concentration and almost not influenced by dust diameter distribution. Actually, small impact of dust diameter variation on transmittance still exists which is one of the main reasons for the relative error in Table 6. Thus, if there exists any, more appropriate optical detection channel should be searched in other bands, like terahertz wave and millimeter wave. (c) The mean diameter of nonuniform particles was set to be 20 μm for the correlation of dust concentration and transmittance. When the diameters of all the particles are greater than the mean diameter (20 μm) by an order of magnitude or more, the transmittance under 1260–1280 cm^{-1} (7.937–7.813 μm) may be changed to be sensitive to the variation of dust diameter which may result in the failure of (11). Such occasion does not exist in underground coal mine for there is a limited range of dust diameter. Special attention should be paid in extreme cases.

6. Conclusions

Aiming at the respirable coal dust pollution in the fully mechanized working face of Huangbaici coal mine, the coal particles were sampled to conduct the industrial analysis and FT-IR test in order to obtain the chemical composition and optical constants of coal particles. The spatial distribution of coal dust in working face was also measured by field measurement method. The variation of dust spatial distribution under different influencing factors of dust sources (intensity of dust release, position of coal cutting, and the wetting of the coal seam) and airflow fields (wind speed and direction of ventilation) was simulated. Based on the optical constants of coal dust obtained from FT-IR experiment, combined with the Mie scattering and heat flux method, the transmission characteristics and AOD of coal dust were analyzed and summarized. Simulation results show that (a) the transmission characteristics of coal dust are greatly decreased with the increasing dust release intensity but are slightly enhanced with the advance of the coal mining activity. The AOD of coal dust is obviously decreased with the wetting of the coal seam. (b) The spectral AODs of coal dust are obviously decreased with increasing wind speeds under the threshold of the optimal wind speed. The AOD of coal dust under negative ventilation is slightly greater than that under positive ventilation.

Furthermore, an optical channel of 1260–1280 cm^{-1} (7.937–7.813 μm) was observed in the transmittance under different influencing factors and further analyzed on its sensitivity of dust diameter variation. The analysis proved that the transmittance of coal dust under the optical channel of 1260–1280 cm^{-1} (7.937–7.813 μm) is almost not influenced by the variation of dust diameter and can be considered as the only function of dust concentration. Then, a fitting function was given based on the correlation of dust concentration and optical transmittance considering the dust pollution level in underground working face. Based on the field measurement data on the dust pollution in this working face, the optical transmittance was calculated and then loaded into the corresponding fitting function in our study to get the retrieved equivalent dust concentration. The field dust concentration and retrieved dust concentration agree well considering the engineering application and all the relative errors are within 0.1. Such method including the optical channel and fitting function can be used for the monitoring of the equivalent dust concentration in the fully mechanized working face of Huangbaici coal mine.

Competing Interests

The authors declare that they have no competing interests.

Acknowledgments

This research is supported by the Outstanding Youth Science Foundation of NSFC (no. 51522601) and Program for New Century Excellent Talents in University (NCET-13-0173).

References

[1] Z. Wang and T. Ren, "Investigation of airflow and respirable dust flow behaviour above an underground bin," *Powder Technology*, vol. 250, pp. 103–114, 2013.

[2] E. Petavratzi, S. Kingman, and I. Lowndes, "Particulates from mining operations: a review of sources, effects and regulations," *Minerals Engineering*, vol. 18, no. 12, pp. 1183–1199, 2005.

[3] S. Su, H. Chen, P. Teakle, and S. Xue, "Characteristics of coal mine ventilation air flows," *Journal of Environmental Management*, vol. 86, no. 1, pp. 44–62, 2008.

[4] R. K. Eckhoff, "Does the dust explosion risk increase when moving from μm-particle powders to powders of nm-particles?" *Journal of Loss Prevention in the Process Industries*, vol. 25, no. 3, pp. 448–459, 2012.

[5] Y. Xue, F. Gao, and X. Liu, "Effect of damage evolution of coal on permeability variation and analysis of gas outburst hazard with coal mining," *Natural Hazards*, vol. 79, no. 2, pp. 999–1013, 2015.

[6] A. M. Donoghue, "Occupational health hazards in mining: an overview," *Occupational Medicine*, vol. 54, no. 5, pp. 283–289, 2004.

[7] D. E. Gildfind and R. G. Morgan, "A new shock tube configuration for studying dust-lifting during the initiation of a coal dust explosion," *Journal of Loss Prevention in the Process Industries*, vol. 29, no. 1, pp. 198–208, 2014.

[8] M. Onder and S. Onder, "Evaluation of occupational exposures to respirable dust in underground coal mines," *Industrial Health*, vol. 47, no. 1, pp. 43–49, 2009.

[9] K. Vizayakumar and P. K. J. Mohapatra, "Environmental impact analysis of a coalfield," *Journal of Environmental Management*, vol. 34, no. 2, pp. 79–103, 1992.

[10] R. Klemens, P. Kosinski, P. Wolanski et al., "Numerical study of dust lifting in a channel with vertical obstacles," *Journal of Loss Prevention in the Process Industries*, vol. 14, no. 6, pp. 469–473, 2001.

[11] J. Toraño, S. Torno, M. Menéndez, and M. Gent, "Auxiliary ventilation in mining roadways driven with roadheaders: validated CFD modelling of dust behaviour," *Tunnelling and Underground Space Technology*, vol. 26, no. 1, pp. 201–210, 2011.

[12] M. Liu, G. Shi, Z. Guo, Y. Wang, and L. Ma, "3-D simulation of gases transport under condition of inert gas injection into goaf," *Heat and Mass Transfer*, 2016.

[13] T. Ren, Z. Wang, and G. Cooper, "CFD modelling of ventilation and dust flow behaviour above an underground bin and the design of an innovative dust mitigation system," *Tunnelling and Underground Space Technology*, vol. 41, no. 1, pp. 241–254, 2014.

[14] S. Wang and J. Hao, "Air quality management in China: issues, challenges, and options," *Journal of Environmental Sciences*, vol. 24, no. 1, pp. 2–13, 2012.

[15] E. Emili, C. Popp, M. Petitta, M. Riffler, S. Wunderle, and M. Zebisch, "PM10 remote sensing from geostationary SEVIRI and polar-orbiting MODIS sensors over the complex terrain of the European Alpine region," *Remote Sensing of Environment*, vol. 114, no. 11, pp. 2485–2499, 2010.

[16] Z. Ruan, Y. Yuan, X. Zhang, Y. Shuai, and H. Tan, "Determination of optical properties and thickness of optical thin film using stochastic particle swarm optimization," *Solar Energy*, vol. 127, pp. 147–158, 2016.

[17] Y. Yuan, Y. Shuai, X.-W. Li, B. Liu, and H.-P. Tan, "Using a new aerosol relative optical thickness concept to identify aerosol particle species," *Atmospheric Research*, vol. 150, pp. 1–11, 2014.

[18] K. Lebecki and M. Małachowski, "Optical method for continuous monitoring of dust deposition in mine's entry," *Archives of Mining Sciences*, vol. 57, no. 3, pp. 517–534, 2012.

[19] P. Lilienfeld and J. Dulchinos, "Portable instantaneous mass monitor for coal mine dust," *American Industrial Hygiene Association Journal*, vol. 33, no. 3, pp. 136–145, 1972.

[20] A. H. Lehocky and P. L. Williams, "Comparison of respirable samplers to direct-reading real-time aerosol monitors for measuring coal dust," *American Industrial Hygiene Association Journal*, vol. 57, no. 11, pp. 1013–1018, 1996.

[21] Y. Liang, H. Liang, and S. Zhu, "Mercury emission from coal seam fire at Wuda, Inner Mongolia, China," *Atmospheric Environment*, vol. 83, pp. 176–184, 2014.

[22] C. Kuenzer, J. Zhang, Y. Sun, Y. Jia, and S. Dech, "Coal fires revisited: The Wuda coal field in the aftermath of extensive coal fire research and accelerating extinguishing activities," *International Journal of Coal Geology*, vol. 102, pp. 75–86, 2012.

[23] S. Dai, D. Ren, Y. Tang, L. Shao, and S. Li, "Distribution, isotopic variation and origin of sulfur in coals in the Wuda coalfield, Inner Mongolia, China," *International Journal of Coal Geology*, vol. 51, no. 4, pp. 237–250, 2002.

[24] W. Z. Wang, Y. M. Wang, and G. Q. Shi, "Forward research on transmission characteristics of near-surface particulate-matter-polluted atmosphere in mining area combined with CFD method," *Optics Express*, vol. 23, no. 15, pp. A1010–A1023, 2015.

[25] H. Liu, *Coal Mine Safety Regulation, Expert Interpretation*, China University of Mining and Technology Press, Xuzhou, China, 2006 (Chinese).

[26] J. Yang, X. Wu, J. Gao, and G. Li, "Surface characteristics and wetting mechanism of respirable coal dust," *Mining Science and Technology*, vol. 20, no. 3, pp. 365–371, 2010.

[27] H. S. G. Tucker, "The particle size of some Witwatersrand mine dust," *British Journal of Applied Physics*, vol. 9, no. 3, pp. 98–102, 1958.

[28] S. E. Allaire and L.-E. Parent, "Size guide number and rosin-rammler approaches to describe particle size distribution of granular organic-based fertilisers," *Biosystems Engineering*, vol. 86, no. 4, pp. 503–509, 2003.

[29] W.-Z. Wang, Y.-M. Wang, G.-Q. Shi, and D.-M. Wang, "Numerical study on infrared optical property of diffuse coal particles in mine fully mechanized working combined with CFD method," *Mathematical Problems in Engineering*, vol. 2015, Article ID 501401, 10 pages, 2015.

[30] W. Z. Wang, Y. M. Wang, and G. Q. Shi, "Experimental investigation on the infrared refraction and extinction properties of rock dust in tunneling face of coal mine," *Applied Optics*, vol. 54, no. 35, pp. 10532–10540, 2015.

[31] X. Huang, X. Chen, Y. Shuai et al., "Heat transfer analysis of solar-thermal dissociation of $NiFe_2O_4$ by coupling MCRTM and FVM method," *Energy Conversion and Management*, vol. 106, pp. 676–686, 2015.

[32] H. Tan, L. Liu, H. Yi, J. Zhao, H. Qi, and J. Tan, "Recent progress in computational thermal radiative transfer," *Chinese Science Bulletin*, vol. 54, no. 22, pp. 4135–4147, 2009.

[33] H.-L. Yi, C.-H. Wang, and H.-P. Tan, "Transient radiative transfer in a complex refracting medium by a modified Monte Carlo simulation," *International Journal of Heat and Mass Transfer*, vol. 79, pp. 437–449, 2014.

[34] L. Ma, F. Wang, C. Wang, C. Wang, and J. Tan, "Monte Carlo simulation of spectral reflectance and BRDF of the bubble layer in the upper ocean," *Optics Express*, vol. 23, no. 19, pp. 24274–24289, 2015.

[35] Y.-S. Sun, J. Ma, and B.-W. Li, "Spectral collocation method for convective-radiative transfer of a moving rod with variable thermal conductivity," *International Journal of Thermal Sciences*, vol. 90, pp. 187–196, 2015.

[36] J. Ma, Y. Sun, B. Li, and H. Chen, "Spectral collocation method for radiative-conductive porous fin with temperature dependent properties," *Energy Conversion and Management*, vol. 111, pp. 279–288, 2016.

[37] Z.-X. Jia, Y. Shuai, S.-D. Xu, and H.-P. Tan, "Optical coherent thermal emission by excitation of magnetic polarition in multilayer nanoshell trimer," *Optics Express*, vol. 23, no. 19, pp. A1096–A1110, 2015.

[38] W. Z. Wang, Y. M. Wang, and G. Q. Shi, "Waveband selection within 400–4000 cm^{-1} of optical identification of airborne dust in coal mine tunneling face," *Applied Optics*, vol. 55, no. 11, pp. 2951–2959, 2016.

[39] P. Sadooghi and C. Aghanajafi, "Two-flux method for transient thermal analysis in a layer of polymer fiber," *Journal of Applied Polymer Science*, vol. 101, no. 4, pp. 2277–2283, 2006.